

Structural and optical characterization of pure and starch-capped ZnO quantum dots and their photocatalytic activity

K. Vidhya · M. Saravanan · G. Bhoopathi ·
V. P. Devarajan · S. Subanya

Received: 14 April 2014 / Accepted: 22 April 2014 / Published online: 15 May 2014
© The Author(s) 2014. This article is published with open access at Springerlink.com

Abstract Among the different types of metal oxides, zinc oxide (ZnO) is a most commonly used metal oxide in a broad variety of applications. In the present investigation, a modified green synthesis route was used to synthesize pure and starch-capped ZnO (ZnO/starch) quantum dots (QDs) and studied their structural and optical characteristics. In this study, hexagonal crystal structure was observed in both pure and ZnO/starch QDs using X-ray diffraction technique. A spherical-shaped surface morphology was found with the size of 5–10 nm using transmission electron microscope technique. The interaction between ZnO QDs and starch molecules was proved via Fourier infra-red spectrometer technique. On the other hand, their fluorescence behaviors were investigated using photoluminescence technique, in that the ZnO/starch QDs showed an

enhanced emission behavior when compared to the pure ZnO QDs. Further, the solar photocatalytic activity of both the ZnO QDs was examined with the dye Rhodamine B (RhB) at the end of 30, 60, 90, and 120 min. In this, ZnO/starch QDs show a good and more decomposition of RhB than pure ZnO QDs. Collectively, in the present study, green synthesis route produced an efficient QDs (pure and ZnO/starch) and it will be very useful for many other QDs. The ZnO/starch QDs are suitable for decomposing the RhB and other toxic organic dyes.

Keywords Zinc oxide · Starch · Green synthesis · Quantum dots · Optical properties · Solar photocatalytic activity

K. Vidhya · G. Bhoopathi (✉)
Nanomaterials Laboratory, Department of Physics, PSG College of Arts and Science, Coimbatore 641 014, Tamil Nadu, India
e-mail: bbiju03@gmail.com

M. Saravanan
Unit of Toxicology, Department of Zoology, Bharathiar University, Coimbatore 641 046, Tamil Nadu, India

M. Saravanan
Bio-Regulatory Chemistry Lab, Department of Biological Environment, College of Agriculture and Life Sciences, Kangwon National University, Chuncheon 200-701, Republic of Korea

V. P. Devarajan
Thin Films and Nanomaterials Laboratory, Department of Physics, Bharathiar University, Coimbatore 641 046, Tamil Nadu, India

S. Subanya
Department of Physics, PSGR Krishnammal College for Women, Coimbatore 641 004, Tamil Nadu, India

Introduction

In the recent research on semiconductor, nanoparticles (NPs)/quantum dots (QDs) have become so important because of their greater potential in opto-electronic devices and biological applications (Coe et al. 2002; Fonoberov and Balandin 2006; Rosenthal et al. 2011; Singh et al. 2012). The optical properties of QDs strongly depend on the inter-dot distance which in turn is due to the quantum size effect (Murray et al. 2000). Typically, zinc oxide (ZnO) is a well-known semiconductor with a wide bandgap (~3.37 eV) having unique optical and bio-compatible properties which make it a better candidate for bio-imaging than metal and chalcogenide NPs (Wu et al. 2008). Some of the methods have been reported earlier for synthesizing the ZnO nanocrystals in aqueous solution but they either involved an alkaline media or an annealing method (Noack and Eychmuller 2002; Jin et al. 2003; Wang et al. 2004; Ristic et al. 2005; Sahdan et al. 2010; Xu and Wang 2011;

Huang and Duan 2014) which makes them unsuitable for biological applications. Further, in this case, using various chemicals may produce toxicity which contaminate the NPs and make them unsuitable for biological applications. In order to use the ZnO nanocrystals for bio-applications, the synthetic process has to meet several requirements that should contain only bio-compatible materials or a suitable surface capping agent with a stable colloidal solution and many more (Li et al. 2007; Ratkovich and Penn 2009).

The chemical capping method is now extensively used in the synthesis of NPs since the concentration of capping molecule controls the particles size as well as protects the particles from coagulation (Templeton et al. 2000). It can be carried out at high or low temperature depending on the reactants (Wing et al. 2012). Indeed, organic molecules capped with inorganic nanostructures introduce a new type of photophysical and photochemical properties resulting from the combinatorial effects of organic and inorganic phases (Wilkes et al. 1985; Levy et al. 2004). For instance, conjugated ZnO nanostructure could extend the absorption band up to the visible region and can play an important role in the photocatalytic degradation which could enhance high photocatalytic activity (Qiu et al. 2008; Sudha et al. 2013). Many methods are available for attaching the polymer chains onto surface of NPs, even though the polydispersed NPs nature serves agglomeration due to lack of effective surface passivation. In order to solve this problem, starch molecule is used as a surface capping agent for stabilizing the NPs and to control the particle size. Previous studies suggest that the starch is used as one of the best candidates in “green” capping agents, and a bio-compatible, biodegradable material and renewable polymer. And also it adopts right-handed helical conformation in aqueous solution, in which the extensive number of hydroxyl groups can facilitate the complexation of metal ions to the molecular matrix (Wei et al. 2004; Babu et al. 2013). Therefore, it provides stable surface passivation and/or protection to prevent the aggregation of particles (Raveendran et al. 2006; Engelbrekt et al. 2009). Nowadays semiconductor NPs are used for photocatalytic degradation of toxic organic compounds due to their unique functions (Hoffmann et al. 1995; Ullah and Dutta 2008). In this case, ZnO has been widely used because of their photoactive in the near-UV areas and need of less power of solar light (Hong et al. 2009; Ali et al. 2013).

Dyes are extensively used in the textile industry and the wastewater effluents containing dyestuffs such as non-fixed dyes, fluorine dyes and azo dyes and their degradation products from these textile industries are one of the major pollutants of the aquatic environment because of their huge volume of production from industries, slow biodegradation and decoloration, and toxicity to various biological organisms (Byrappa et al. 2006; Kyung et al.

2005; Zhang 2012). In recent years, available techniques are not completely removed and degraded from the different types of dyes. Therefore, the removal of such dyes from the aquatic system is extremely important and remains a challenge (Bunhu et al. 2011). For instance, Rhodamine B (RhB) is a xanthene dye which is widely used as a colorant in textiles and food stuffs, and also in water tracer fluorescent. It causes many health-related harmful effects such as irritation to the skin, eyes and respiratory tract. It produces carcinogenicity, reproductive and developmental toxicity, neurotoxicity and chronic toxicity to humans and animals (Jain et al. 2007). Consequently, the present study was aimed to develop an easy, environment friendly and cost-effective ZnO QDs by a “green” synthesis route using starch as capping agent. More importantly, the photoluminescence (PL) and photocatalytic activities in RhB dye of both pure ZnO and ZnO/starch QDs were investigated.

Materials and methods

Chemicals

All chemicals used were of standard analytical grade (AR) and not further treated. Zinc acetate ($\text{Zn}(\text{CH}_3\text{COO})_2$), sodium hydroxide (NaOH) and starch are the precursors with the solvent of double distilled water (DDW). RhB dye was used for photocatalytic degradation study. The detailed sample preparation techniques are described as follows.

Preparation of QDs

For the synthesis of ZnO QDs, 0.05 mol of $\text{Zn}(\text{CH}_3\text{COO})_2$ solution was freshly prepared to which freshly prepared NaOH (base solution) was slowly added in drops till the pH reaches 10. The mixture solution was stirred vigorously until a white color colloidal solution was formed. Further, the solution was treated under ultrasonic condition for stabilization of particles. Finally, the solution was stored without any annoyance so that the particles get sedimented. The sedimentation was washed several times for removing the unreacted compounds and then it was centrifuged at 10,000 rpm for 20 min. After that, the particles were separated from the solution and then dried in vacuum desiccator. Further, collected crystal sample was oxidized through annealing treatment and grinded well. Finally, a white color ZnO powder was obtained and used for further analysis. For ZnO/starch QDs, the same procedure was performed but the capping agent of starch (as monolayer) was added in drops into the $\text{Zn}(\text{CH}_3\text{COO})_2$ solution before changing the pH value. Finally, the prepared samples were analyzed under various characterization techniques.

Preparation of photocatalysts

For photocatalysis analysis, 0.03 mol of RhB dye was dissolved in 50 ml of DDW and stirred well under dark condition. Then, 9 mg/50 ml of each QD sample was dispersed in the dye solution and stirred well to make a complex formation between QDs and dye. The catalytic sample solutions were taken in the petri dishes and then placed them under solar light for degradation. The whole experiment was done under solar light environment condition (Wu et al. 2012). The each irradiated sample was collected between the specific time intervals of 30 min such as 30, 60, 90 and 120 min and then used for UV absorption measurement to know the decomposition effects.

Results and discussion

Structural analysis

In this study, both pure ZnO QDs and ZnO/starch QDs have shown the hexagonal crystal structure confirmed through XRD patterns (Fig. 1a, b) of powder XRD technique (X'pert PRO model) with $\text{CuK}\alpha$ radiation ($\lambda = 1.54809 \text{ \AA}$) at room temperature. The hexagonal (wurtzite) crystal nature is in close agreement with the standard values (JCPDS card: 36-1451). In the case of ZnO/starch QDs, no major change was observed due to the effect of starch because of its chemical composition (Djokic et al. 2008), but a slight variation was observed in the peak broadening and intensity. The peak broadening clearly indicates the formation of small sized particles than that of ZnO QDs (Choi et al. 2003). Finally, Debye-

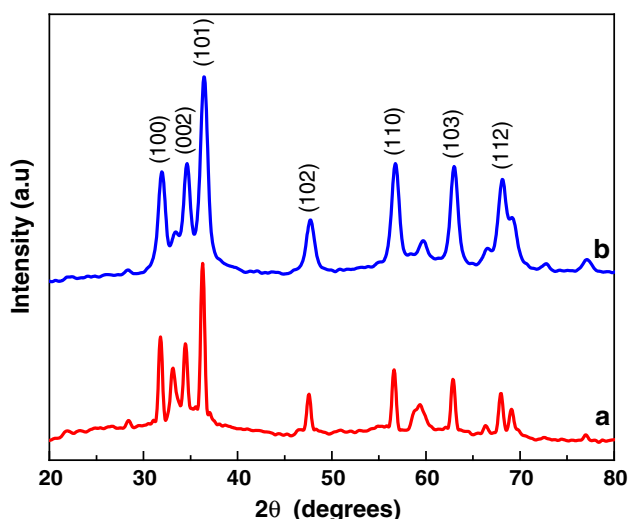


Fig. 1 XRD patterns of pure ZnO QDs (a) and ZnO/starch QDs (b)

Sherrer's formula was used to estimate the crystalline size (D ; average particle size) (Cullity 1978) of both the QD samples which were 15 and 10 nm, and their calculated lattice constant values which were 2.4741 and 2.4636 \AA , respectively.

TEM (model: JEM-2010) images of both the pure and ZnO/starch QDs were presented in Fig. 2a, b, respectively. A spherical-shaped particle nature was observed in the ZnO QDs whose size was nearly 5–10 nm (image a), where slightly elongated particles with little agglomeration were also observed which may be due to the powder samples embedded on the copper-coated grid (Klaumunzer et al. 2014). Whereas in the case of ZnO/starch QDs, it shows spherical-shaped particle nature but cluster-like surface morphology was observed because ZnO QDs are embedded inside the polymer-like starch matrix (image b). Hence, it clearly shows the formation of monodispersed particles and we confirm that this was due to the capping effect of starch molecule. A similar type of morphology was observed as early in the starch-capped CdSe nanostructures (Oluwafemi 2009) and this report highly supports the results of this TEM results. The calculation of particle size was difficult due to its clustered morphology. Consequently, it may be approximately ± 5 nm and, therefore, we confirmed that the size of the both of the QDs lies in QDs scale region. The elemental composition of ZnO and ZnO/starch QDs was confirmed using energy dispersive X-ray analysis (EDAX) technique (model: FEI Quanta 200). In this study, Fig. 3a and b shows the EDAX spectrum of pure ZnO and ZnO/starch QDs. From this analysis, it is confirmed that the presence of elements and their corresponding composition values were found to be $\text{Zn}_{66}\text{O}_{34}$ and Zn_{96}O_4 , respectively. In the case of ZnO/starch QDs, an unknown peak (* symbol indicated in figure) was observed and we believed the presence of starch molecule on it which is responsible for the formation of monodispersed particle nature.

The chemical structure and interaction between the ZnO QDs and starch molecule were confirmed using KBr mode Fourier infra-red spectrometer (FTIR) spectrum (model: Bruker Tensor-27). The FTIR spectrum of pure ZnO QDs (a), ZnO/starch QDs (b) and starch molecule (c) was given in Fig. 4a–c, respectively. In this study, the broad band located between 400 and 550 cm^{-1} was attributed due to the Zn–O stretching mode and the other bands are corresponding to the stretching vibration of O–H bond and $1,410 \text{ cm}^{-1}$ was due to asymmetric and symmetric stretching vibration of carbonyl group (COO–Zn coordination) (Jiang et al. 2008). For the comparison purpose, starch molecule FTIR spectrum was recorded. Naturally, starch molecule contains many of O–H functional groups (Tomasik and Schilling 2004), further these are easy to bind with the metal surface. The major peaks at

Fig. 2 TEM images of pure ZnO QDs (a) and ZnO/starch QDs (b)

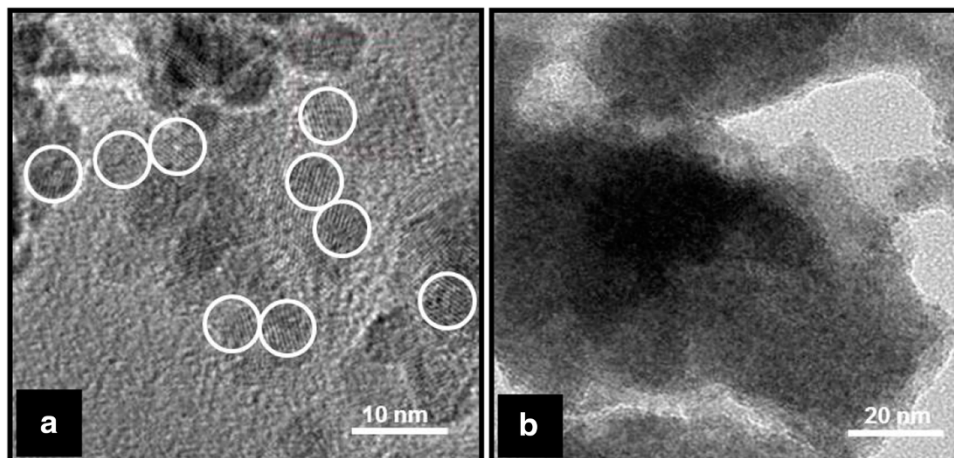


Fig. 3 EDAX spectrum of pure ZnO QDs (a) and ZnO/starch QDs (b)

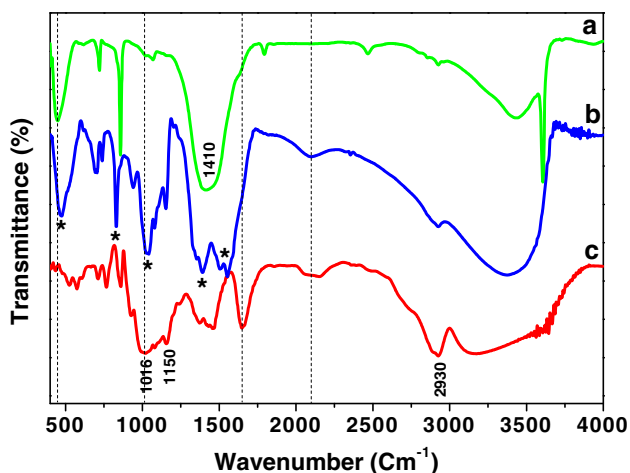
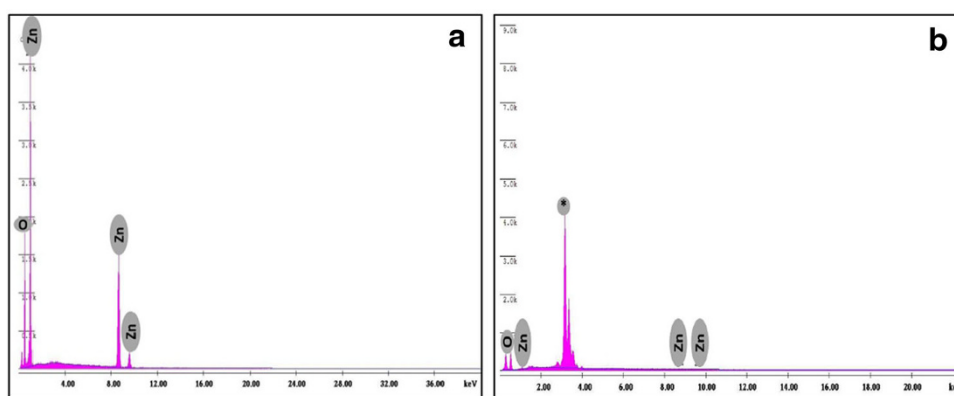


Fig. 4 FTIR spectrum of pure ZnO QDs (a), ZnO/starch QDs (b) and starch (c)

1,150 cm^{-1} (C–O–H group), 1,080 and 1,016 cm^{-1} (C–O–C group) were due to the anhydroglucose ring of starch and 2,930 cm^{-1} was characteristic of C–H stretching associated with ring methane hydrogen atoms (Ma et al. 2009; Zamari et al. 2012). And other peaks are corresponding to 766 cm^{-1} (C–C stretching), 860 cm^{-1} (C–C, CH_2

deformation), 1,428 cm^{-1} (CH_2 bending), 1,646 cm^{-1} (O–H bending of water absorbance) and 2,930 cm^{-1} (CH_2 deformation and C–O–O stretching), respectively. In case of starch-capped ZnO QDs, the appearance/disappearance (** symbol indicated in the graph) and shifting (* symbol indicated in the graph) of peaks confirm the bond formation between ZnO QDs and soluble starch molecule, where covalent bond was not formed between ZnO QDs and starch molecule which was confirmed from the previous report (Vigneshwaran et al. 2006).

Optical analysis

In the present study, Fig. 5 shows the UV absorption spectrum (UV–VIS–NIR spectrophotometer, Shimatzu 3600 model) of pure ZnO (a) and ZnO/starch (b) QDs, the direct band to band transition has occurred and their calculated corresponding bandgap energy values was approximately 3.8 eV (320 nm) calculated using $E = hc/\lambda$ formula. A similar observation was also found by the previous reports (Irimpan et al. 2007; Klingshirn 2007), which hold well with our results. In the case of ZnO/starch QDs, a little red shift and enhanced absorption was observed in the peak position when compared with ZnO

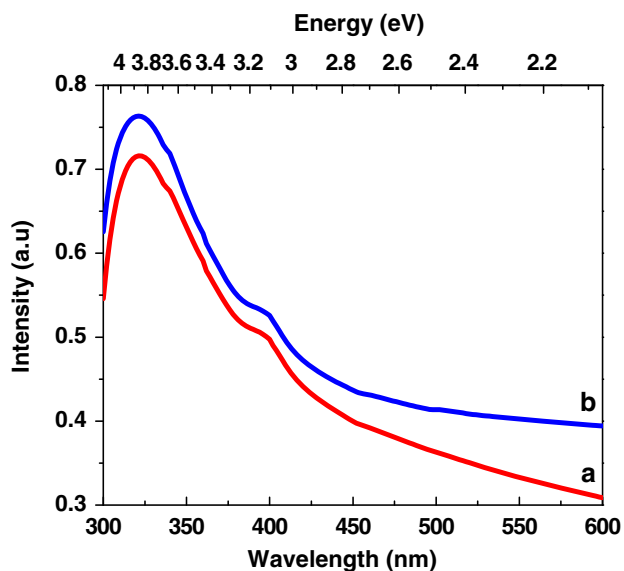


Fig. 5 UV absorption spectrum of pure ZnO QDs (a) and ZnO/starch QDs (b)

QDs. Therefore, it is believed that this shift was due to the encapsulation effect of starch molecule around the ZnO crystals and it might be a reason for the formation of cluster-like morphology (Mercedes et al. 2006) which goes well with our TEM results (clustered morphology in ZnO/starch QDs).

The PL emission behaviors of both pure ZnO and ZnO/starch QDs were measured by spectrofluorometer (Spectrofluoromax-4 model) and excited at 325 nm (Fig. 6a, b). From the pure ZnO QDs, we observed a violet emission peak at 365 nm assigned near band-edge emission arising from the recombination of trapped electron–hole pairs and additionally an oxygen vacancy-related visible green emission band at 550 nm was also observed. These emission behaviors are believed that whenever quantum confinement takes place their bandgap nature changes from indirect to direct bandgap (Sun et al. 2008; Hu and Chen 2008; Yang et al. 2008). Usually, bulk ZnO does not show this much of luminescence behavior because of their indirect bandgap nature (Studenikin et al. 2000). When having direct bandgap for capped/doped materials, wider PL is possible, whereas from the ZnO/starch QDs, we have observed an interesting broad blue emission spectrum from violet to green region, maximum at 440 nm which is due to the recombination electrons being trapped in random surface holes. In this case, near band-edge and oxygen vacancy-related emission behaviors are quenched due to the surface passivation and thus enhanced the blue emission because small sizes of ZnO QDs are formed inside the starch matrix (Malik et al. 2014) (see TEM result of ZnO/starch QDs). Our opinion is that this type of blue emission behavior is an interesting one. In this case, so far a few

reports were documented in relation to ZnO/starch NPs. This emission nature might be attributed due to the smaller particles that adhered together to form elongated particles (Vigneshwaran et al. 2006; Chandramouleeswaran et al. 2007; Prasad et al. 2010). Further, color emissions of these QDs were confirmed through fluorescence images under UV light source using fluorescence microscope (Fig. 7a, b).

Photocatalysis analysis

The photocatalytic activity of both the QDs was characterized by the degradation activity of RhB dye. In the photocatalysis process, UV light-absorbed QDs promote the electrons from valance band (VB) to conduction band (CB) and the outcome of this process is a region of positive charge holes (h^+) in the valance band (VB) and negative charge electrons (e^-) in the conduction band (CB) as



The leaving holes in the VB react with the hydroxylated surface to produce $\cdot\text{OH}$ radicals which are the most potent oxidizing agents and the degradation rate confirms the potency of the $\cdot\text{OH}$ radical. The photo-generated electrons react with the molecular oxygen (O_2) to produce superoxide radical anions ($\cdot\text{O}_2^-$) and then photo-generated holes react with water to produce hydroxyl ($\cdot\text{OH}$) radicals. These reactive radicals are then responsible for the degradation of organic compounds with QDs (Turchi and Ollis 1990; Pouretedal et al. 2010). In this study, at the end of each interval time, the color difference in the irradiated dye solution of both pure and ZnO/starch QDs was observed and it confirms degradation of RhB dye, whereas no observable dye degradation in RhB dye solution was found after irradiation. Therefore, we conclude that the effect of degradation was due to the presence of QDs in the RhB dye solution under solar light environment (Fig. 8 a–d). In this case, the absorption spectrum for solar photocatalytic activity of both the pure ZnO and ZnO/starch QDs was presented in Fig. 9a, b, respectively. The absorption spectrum of RhB dye was measured first and it shows the maximum absorption in the visible region which is at 550 nm and also a minimum absorption in the UV region. Further, all the irradiated samples show a higher photocatalytic activity around 550 nm (Nagaraja et al. 2012) where their absorption intensity decreases slowly with increase in the irradiation time which indicates the degradation of the dye (Ali et al. 2013). Due to the formation of more free-radical from small size of QDs, a higher degradation effect was observed in the ZnO/starch QDs corresponding to that of pure ZnO QDs (Qiu et al. 2008).

Fig. 6 PL emission spectrum of ZnO QDs (a) and ZnO/starch QDs (b)

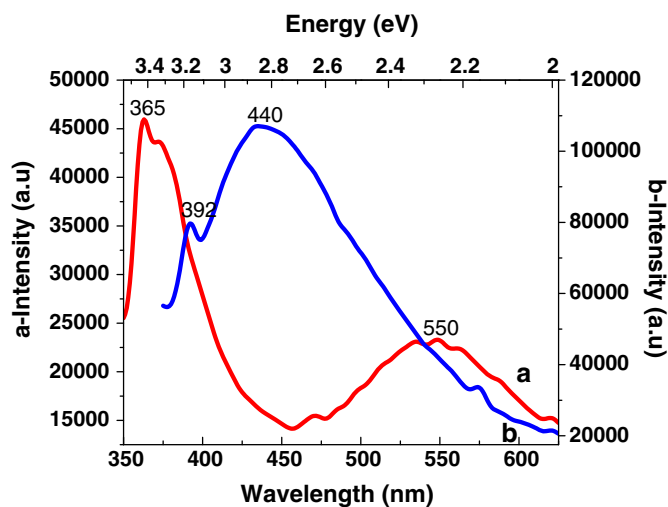


Fig. 7 Fluorescence images of pure ZnO QDs (a) and ZnO/starch QDs (b) under UV light

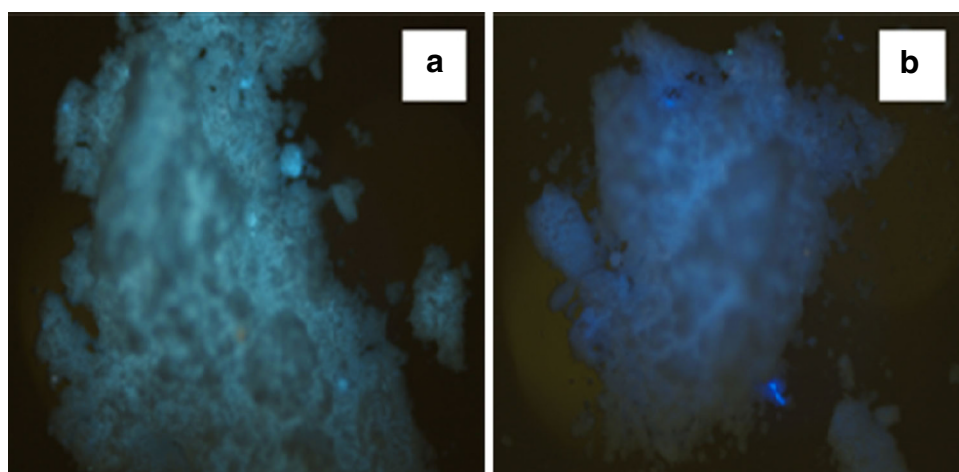


Fig. 8 Photographic images for solar photodegradation of RhB dye before irradiation (a), RhB dye after irradiation (120 min) (b), pure ZnO QDs with RhB after irradiation (120 min) (c) and ZnO/starch QDs with RhB after irradiation (120 min) (d)

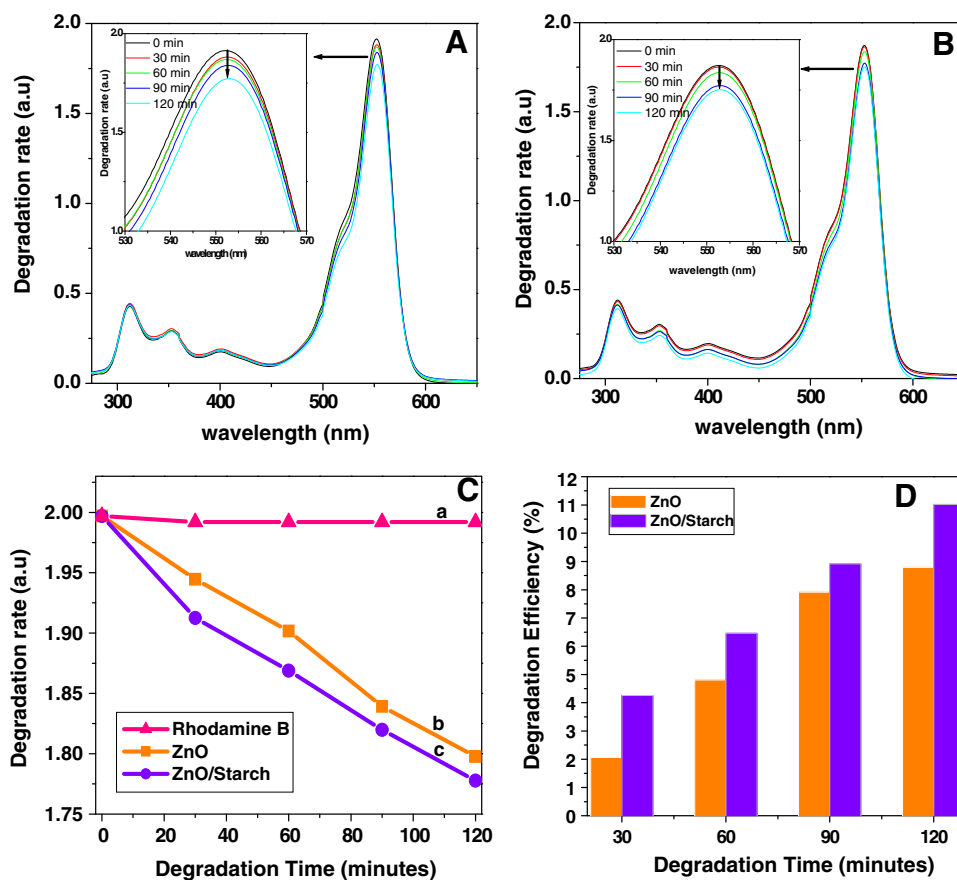
The photodegradation comparison spectrum was plotted as a relation between irradiation time and absorption intensity in Fig. 9c. The degradation percentage of the dye was determined (Fig. 9d) in terms of change in maximum

absorption intensity before and after irradiation and it was calculated using the following formula (Khayyat et al. 2012).

$$D(\%) = \frac{(A_0 - A_t)}{A_0} \times 100$$

where D is the degradation efficiency of dye or dye removal efficiency (in percentage), A_0 is the absorption of dye maximum before irradiation (in 0 min) and A_t is the absorption of dye maximum after irradiation (t in minutes). These results confirm the red shift in UV absorption spectrum (Fig. 5a, b) and also support the decrement of bandgap energy corresponding to the samples results without photocatalytic action. Hence, the results show less degradation efficiency (approximately 11 %) even though we have achieved ZnO/starch QDs photodegradation of dye under solar light environment because this type of photodegradation can be suitable to remove the contamination from the river water. But this degradation efficiency will be increased with increased irradiation time and also it may show increased degradation rate. The results of this

Fig. 9 Solar photodegradation spectrum of RhB dye in pure ZnO QDs (a), ZnO/starch QDs (b), photodegradation rate of QDs with control (RhB dye) (c) and photodegradation efficiency of QDs (d)



study indicate that the photocatalytic activity of ZnO:starch QDs was much higher than that of pure ZnO QDs. Similarly, Shi et al. (2011) and Zhang (2013) found a very good photocatalytic degradation of RhB dye with TiO₂ NPs.

Conclusions

In the present investigation, a modified precipitate green synthesis route was used to prepare the pure ZnO and ZnO/starch QDs because of its mild, simple and efficient green route for producing the QDs. In this study, the XRD results show the hexagonal crystal structure and TEM images indicate 5–10 nm spherical-shaped particles. Further, the FTIR studies confirm the interaction between ZnO QDs and starch molecule. In the PL analysis, an interesting strong and broad blue emission was observed in ZnO/starch QDs which is entirely different from the pure ZnO QDs. And also, the solar photocatalytic activity of the ZnO/starch QDs shows the enhanced degradation of the RhB dye. Consequently, the results of the present study are concluded that a modified precipitate green synthesis route is a valuable method for the synthesis of both the pure ZnO and ZnO/starch QDs. Among these QDs, ZnO/starch QDs have a potential photocatalytic

degradation of RhB dye compared to the pure ZnO QDs and it may be useful for variety of dyes present in the effluent discharged from various industries. However, more detailed studies on these aspects are needed and to be elucidated.

Acknowledgments The author K. Vidhya would like to thank and acknowledge the University Grants Commission (UGC), Government of India for providing the financial support to carry out the project work. Fellowship award letter no: F1-17.1/2012-13/RGNF-2012-13-SC-TAM-33174/(SA-III/Website), dated: 28.02.2013. The author (KV) would also like to thank Dr. D. Nataraj, Assistant Professor in Physics, Bharathiar University, Coimbatore, Tamil Nadu, India for providing permission to use the PL analysis.

Open Access This article is distributed under the terms of the Creative Commons Attribution License which permits any use, distribution, and reproduction in any medium, provided the original author(s) and the source are credited.

References

- Ali MA, Idris MR, Quayum ME (2013) Fabrication of ZnO nanoparticles by solution-combustion method for the photocatalytic degradation of organic dye. *J Nanostruc Chem* 3(36):1–6
- Babu PR, O'Connor K, Seeram R (2013) Current progress on bio-based polymers and their future trends. *Prog Biomater* 2(8):1–16

- Bunhu T, Kindness A, Martincigh BS (2011) Determination of titanium dioxide in commercial sunscreens by inductively coupled plasma-optical emission spectrometry. *S Afr J Chem* 64:139–143
- Byrappa K, Subramani AK, Ananda S, Lokanatha Rai KM, Dinesh R, Yoshimura M (2006) Photocatalytic degradation of Rhodamine B dye using hydrothermally synthesized ZnO. *Bull Mater Sci* 29:433–438
- Chandramouleeswaran S, Mhaske ST, Kathe AA, Varadarajan PV, Prasad V, Vigneshwaran N (2007) Functional behaviour of polypropylene/ZnO-soluble starch nanocomposites. *Nanotechnol* 18(385702):1–8
- Choi HH, Ollinger M, Singh RK (2003) Enhanced cathodoluminescent properties of ZnO encapsulated ZnS:Ag phosphors using an electrochemical deposition coating. *Appl Phys Lett* 82:2494–2496
- Coe S, Woo WK, Bawendi M, Bulovic V (2002) Electroluminescence from single monolayers of nanocrystals in molecular organic devices. *Nature* 420:800–803
- Cullity BD (1978) *Elements of X-ray diffraction*, 2nd edn. Addison-Wesley, Reading, p 102
- Djokic DM, Stern WB, Taubert A (2008) Zinc oxide/carbohydrate hybrid materials via mineralization of starch and cellulose in the strongly hydrated ionic liquid tetrabutylammonium hydroxide. *Cryst Growth Design* 8:330–335
- Engelbrekt C, Sorensen KH, Zhang J, Welinder AC, Jensen PS, Ulstrup J (2009) Green synthesis of gold nanoparticles with starch-glucose and application in bioelectrochemistry. *J Mater Chem* 19:7839–7847
- Fonoberov VA, Balandin AA (2006) ZnO quantum dots: physical properties and optoelectronic applications. *J Nanoelect Optoelect* 1:19–38
- Hoffmann MR, Martin ST, Choi W, Bahnemann DW (1995) Environmental applications of semiconductor photocatalysis. *Chem Rev* 95:69–96
- Hong RY, Li JH, Chen LL, Liu DQ, Li HZ, Zheng Y, Ding J (2009) Synthesis, surface modification and photocatalytic property of ZnO nanoparticles. *J Powder Technol* 189:426–432
- Hu Y, Chen HJ (2008) Preparation and characterization of nanocrystalline ZnO particles from a hydrothermal process. *J Nanopart Res* 10:401–407
- Huang C, Duan X (2014) Simple and rapid preparation of spherical flower-like ZnO and their photocatalytic property. *Phys Status Solidi A*. doi:10.1002/pssa.201330677
- Irimpan L, Nampoori VPN, Radhakrishnan P, Deepthy A, Krishnan B (2007) Size dependent fluorescence spectroscopy of nanocolloids of ZnO. *J App Phys* 102(063524):1–6
- Jain R, Mathur M, Sikarwar S, Mittal A (2007) Removal of the hazardous dye Rhodamine B through photocatalytic and adsorption treatments. *J Environ Manag* 85:953–964
- Jiang Z, Huang Z, Yang P, Chen J, Xin Y, Xu J (2008) High PL efficiency of nanocrystalline/PPV composite nanofibers. *Compos Sci Technol* 68:3240–3244
- Jin CF, Yuan X, Ge WW, Hong JM, Xin XQ (2003) Synthesis of ZnO nanorods by solid state reaction at room temperature. *Nanotechnol* 14:667–669
- Khayyat SA, Akhtar MS, Umar A (2012) ZnO nanocapsules for photocatalytic degradation of thionine. *Mater Lett* 81:239–241
- Klaumunzer M, Distaso M, Hubner J, Mackovic M, Spiecker E, Kryschi C, Peukert W (2014) ZnO superstructures via oriented aggregation initiated in a block copolymer melt. *Cryst Eng Comm* 16:1502–1513
- Klingshirn C (2007) ZnO: from basics towards applications. *Phys Status Solidi (b)* 244:3027–3073
- Kyung H, Lee J, Choi W (2005) Simultaneous and synergistic conversion of dyes and heavy metal ions in aqueous TiO₂ suspensions under visible-light illumination. *Environ Sci Technol* 39:2376–2382
- Levy R, Thanh NTK, Doty RC, Hussain I, Nichols RJ, Schiffrin DJ, Brust M, Fernig DG (2004) Rational and combinatorial design of peptide capping ligands for gold nanoparticles. *J Am Chem Soc* 126:10076–10084
- Li M, Bala H, Lv X, Ma X, Sun F, Tang L, Wang Z (2007) Direct synthesis of monodispersed ZnO nanoparticles in aqueous solution. *Mater Lett* 61:690–693
- Ma X, Chang PR, Yang J, Yu J (2009) Preparation and properties of glycerol plasticized-pea starch/zinc oxide-starch bionanocomposites. *Carbohydr Polym* 75:472–478
- Malik P, Shankar R, Malik V, Sharma N, Mukherjee TK (2014) Green chemistry based benign routes for nanoparticle synthesis. *J Nanopart* 2014:14
- Mercedes A, Esther C, Vicente F, Hermenegildo G (2006) Enhanced photocatalytic activity of zeolite-encapsulated TiO₂ clusters by complexation with organic additives and N-doping. *Chem Phys Chem* 7:200–205
- Murray CB, Kagan CR, Bawendi MG (2000) Synthesis and characterization of monodisperse nanocrystals and close-packed nanocrystal assemblies. *Annu Rev Mater Sci* 30:545–610
- Nagaraja R, Kottam N, Girija CR, Nagabhushana BM (2012) Photocatalytic degradation of Rhodamine B dye under UV/solar light using ZnO nanopowder synthesized by solution combustion route. *Powder Technol* 215–216:91–97
- Noack V, Eychmuller A (2002) Annealing of nanometer-sized zinc oxide particles. *Chem Mater* 14:1411–1417
- Oluwafemi OS (2009) A novel “green” synthesis of starch-capped CdSe nanostructures. *Colloid Surf B Biointerfaces* 73:382–386
- Pouretedal HR, Beigy H, Keshavarz MH (2010) Bleaching of Congo red in the presence of ZnS nanoparticles, with dopant of Co²⁺ ion, as photocatalyst under UV and sunlight irradiations. *Environ Technol* 31:1183–1190
- Prasad V, Shaikh AJ, Kathe AA, Bisoyi DK, Verma AK, Vigneshwaran N (2010) Functional behaviour of paper coated with zinc oxide-soluble starch nanocomposites. *J Mater Proc Technol* 210:1962–1967
- Qiu R, Zhang D, Mo Y, Song L, Brewer E, Huang X, Xiong Y (2008) Photocatalytic activity of polymer-modified ZnO under visible light irradiation. *J Hazard Mater* 156:80–85
- Ratkovich A, Penn RL (2009) Zinc oxide nanoparticle growth from homogenous solution: influence of Zn:OH, water concentration, and surfactant additives. *Mater Res Bull* 44:993–998
- Raveendran P, Fua J, Scott L (2006) A simple and green method for the synthesis of Au, Ag, and Au–Ag alloy nanoparticles. *Green Chem* 8:34–38
- Ristic M, Music S, Ivanda M, Popovic S (2005) Sol–gel synthesis and characterization of nanocrystalline ZnO powders. *J Alloy Comp* 397:L1–L4
- Rosenthal SJ, Chang JC, Kovtun O, McBride JR, Tomlinson ID (2011) Biocompatible quantum dots for biological applications. *Chem Biol* 18:10–24
- Sahdan MZ, Mamat MH, Salina M, Khusaimi Z, Noor UM, Rusop M (2010) Heat treatment effects on the surface morphology and optical properties of ZnO nanostructures. *Phys Status Solidi C* 7:2286–2289
- Shi X, Yang X, Wang S, Wang S, Zhang Q, Wang Y (2011) Photocatalytic degradation of Rhodamine B dye with high purity anatase nano-TiO₂ synthesized by a hydrothermal method. *J Wuhan Univ Technol Mater Sci Ed* 26:600–605
- Singh N, Mehra RM, Kapoor A, Soga T (2012) ZnO based quantum dot sensitized solar cell using CdS quantum dots. *J Renew Sustain Energ* 4(013110):1–10
- Studenikin SA, Cocivera M, Kellner W, Pascher H (2000) Band-edge photoluminescence in polycrystalline ZnO films at 1.7 K. *J Lumines* 91:223–232

- Sudha M, Senthilkumar S, Hariharan R, Suganthi A, Rajarajan M (2013) Synthesis, characterization and study of photocatalytic activity of surface modified ZnO nanoparticles by PEG capping. *J Sol Gel Sci Technol* 65:301–310
- Sun D, Sue HJ, Miyatake N (2008) Optical properties of ZnO quantum dots in epoxy with controlled dispersion. *J Phys Chem* 112:16002–16010
- Templeton AC, Wuelfing WP, Murray RW (2000) Monolayer-protected cluster molecules. *Acc Chem Res* 33:27–36
- Tomasiak P, Schilling CH (2004) Chemical modification of starch. *Adv Carbohydr Chem Biochem* 59:175–403
- Turchi CS, Ollis DF (1990) Photocatalytic degradation of organic water contaminants: mechanisms involving hydroxyl radical attack. *J Catal* 122:178–192
- Ullah R, Dutta J (2008) Photocatalytic degradation of organic dyes with manganese-doped ZnO nanoparticles. *J Hazard Mater* 156:194–200
- Vigneshwaran N, Kumar S, Kathe AA, Varadarajan PV, Prasad V (2006) Functional finishing of cotton fabrics using zinc oxide-soluble starch nanocomposites. *Nanotechnol* 17:5087–5095
- Wang Z, Qian XF, Yin J, Zhu Z-K (2004) Large-scale fabrication of tower-like, flower-like, and tube-like ZnO arrays by a simple chemical solution route. *Langmuir* 20:3441–3448
- Wei Q, Kang SH, Mu J (2004) Green synthesis of starch capped CdS nanoparticles. *Colloids Surf A Physicochem Eng. Asp* 247:125–127
- Wilkes GL, Orlor B, Huang HH (1985) Ceramics: hybrid materials incorporating polymer/oligomeric species into inorganic glasses utilizing a sol-gel approach. *Polym Prep* 26:300–301
- Wing CG, Salazar JJV, Yacaman MJ (2012) Procedures for the synthesis and capping of metal nanoparticles. *Methods Mol Biol* 906:3–19
- Wu YL, Fu S, Tok AIY, Zeng XT, Lim CS, Kwek LC, Boey FCY (2008) A dual-colored bio-marker made of doped ZnO nanocrystals. *Nanotechnol* 19(345605):1–9
- Wu M, Yan JM, Zhao M, Jiang Q (2012) Facile synthesis of an Ag₂O–ZnO nanohybrid and its high photocatalytic activity. *Chem Plus Chem* 00:1–6
- Xu S, Wang ZL (2011) One-dimensional ZnO nanostructures: solution growth and functional properties. *Nano Res* 4:1013–1098
- Yang Y, Sun XW, Tay BK, Cao PHT, Wang JX, Zhang XH (2008) Revealing the surface origin of green band emission from ZnO nanostructures by plasma immersion ion implantation induced quenching. *J Appl Phys* 103(064307):1–4
- Zamari R, Zakaria A, Ahangar HA, Darroudi M, Zak A, Drummen GPC (2012) Aqueous starch as a stabilizer in zinc oxide nanoparticles synthesis via laser ablation. *J Alloy Comp* 516:41–48
- Zhang DF (2012) Effects of deposited metallic Silver on nano-ZnO for the environmental purification of dye pollutants. *S Afr J Chem* 65:98–103
- Zhang D (2013) Removal of cationic Rhodamine B dye using nanotitanium with anatase crystalline structure and kinetic analysis of the photocatalytic reaction. *Rus J Phys Chem A* 87:129–136